

See discussions, stats, and author profiles for this publication at: <https://www.researchgate.net/publication/260606721>

Effective Antifouling Using Quorum-Quenching Acylase Stabilized in Magnetically-Separable Mesoporous Silica

ARTICLE in BIOMACROMOLECULES · MARCH 2014

Impact Factor: 5.75 · DOI: 10.1021/bm401595q · Source: PubMed

CITATIONS

9

READS

75

7 AUTHORS, INCLUDING:



Kyung-Min Yeon

Samsung

19 PUBLICATIONS 706 CITATIONS

[SEE PROFILE](#)



Jongmin Shim

S K C

13 PUBLICATIONS 248 CITATIONS

[SEE PROFILE](#)



Kim Sang ryoung

Yale University

12 PUBLICATIONS 182 CITATIONS

[SEE PROFILE](#)



Jungbae Kim

Korea University

108 PUBLICATIONS 3,961 CITATIONS

[SEE PROFILE](#)

Effective Antifouling Using Quorum-Quenching Acylase Stabilized in Magnetically-Separable Mesoporous Silica

Byoungsoo Lee,^{†,‡} Kyung-Min Yeon,^{†,§} Jongmin Shim,^{||} Sang-Ryoung Kim,[§] Chung-Hak Lee,[§] Jinwoo Lee,^{||} and Jungbae Kim^{*,†,‡}

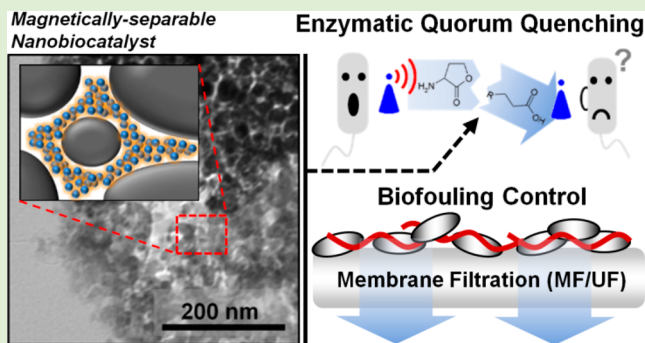
[†]Department of Chemical and Biological Engineering, Korea University, Seoul 136-701, Korea

[§]School of Chemical and Biological Engineering, Seoul National University, Seoul 151-744, Korea

^{||}Department of Chemical Engineering, Pohang University of Science and Technology, Pohang 790-784, Korea

Supporting Information

ABSTRACT: Highly effective antifouling was achieved by immobilizing and stabilizing an acylase, disrupting bacterial cell-to-cell communication, in the form of cross-linked enzymes in magnetically separable mesoporous silica. This so-called “quorum-quenching” acylase (AC) was adsorbed into spherical mesoporous silica (S-MPS) with magnetic nanoparticles (Mag-S-MPS), and further cross-linked for the preparation of nanoscale enzyme reactors of AC in Mag-S-MPS (NER-AC/Mag-S-MPS). NER-AC effectively stabilized the AC activity under rigorous shaking at 200 rpm for 1 month, while free and adsorbed AC lost more than 90% of their initial activities in the same condition within 1 and 10 days, respectively. When applied to the membrane filtration for advanced water treatment, NER-AC efficiently alleviated the biofilm maturation of *Pseudomonas aeruginosa* PAO1 on the membrane surface, thereby enhancing the filtration performance by preventing membrane fouling. Highly stable and magnetically separable NER-AC, as an effective and sustainable antifouling material, has a great potential to be used in the membrane filtration for water reclamation.



INTRODUCTION

Biofouling, representing the formation of cell aggregates within a glue-like slime matrix (biofilm), has attracted a great deal of attention due to its negative effects in various fields, such as medical implants, ship hulls, biosensors, and water treatment facilities.^{1–4} One of the important mechanisms for biofilm formation is quorum sensing (QS), regulating bacterial physiology by small signaling molecules, called autoinducers.⁵ When the autoinducer concentration goes beyond its threshold, it activates the transcription of specific genes to induce the group behaviors such as bioluminescence, antibiotic production, virulence, biofilm, and sporulation.^{6–9} One of well-studied autoinducers is *N*-acyl-homoserine lactones (AHLs), consisting of a homoserine lactone ring and an amide (*N*)-linked acyl side chain with 4–18 carbons.¹⁰ QS based on AHLs can be controlled in various ways, such as blockage of AHL production, interference of AHL interaction with receptor proteins, and inactivation of AHL molecules. Of these QS control strategies, enzymatic degradation of AHLs using acylase or lactonase is one of good candidates for highly effective and sustainable antifouling platform. According to recent reports, acylase from porcine kidney effectively alleviates the biofouling of membranes for wastewater treatment and desalination, thereby enhancing the membrane filterability to a large

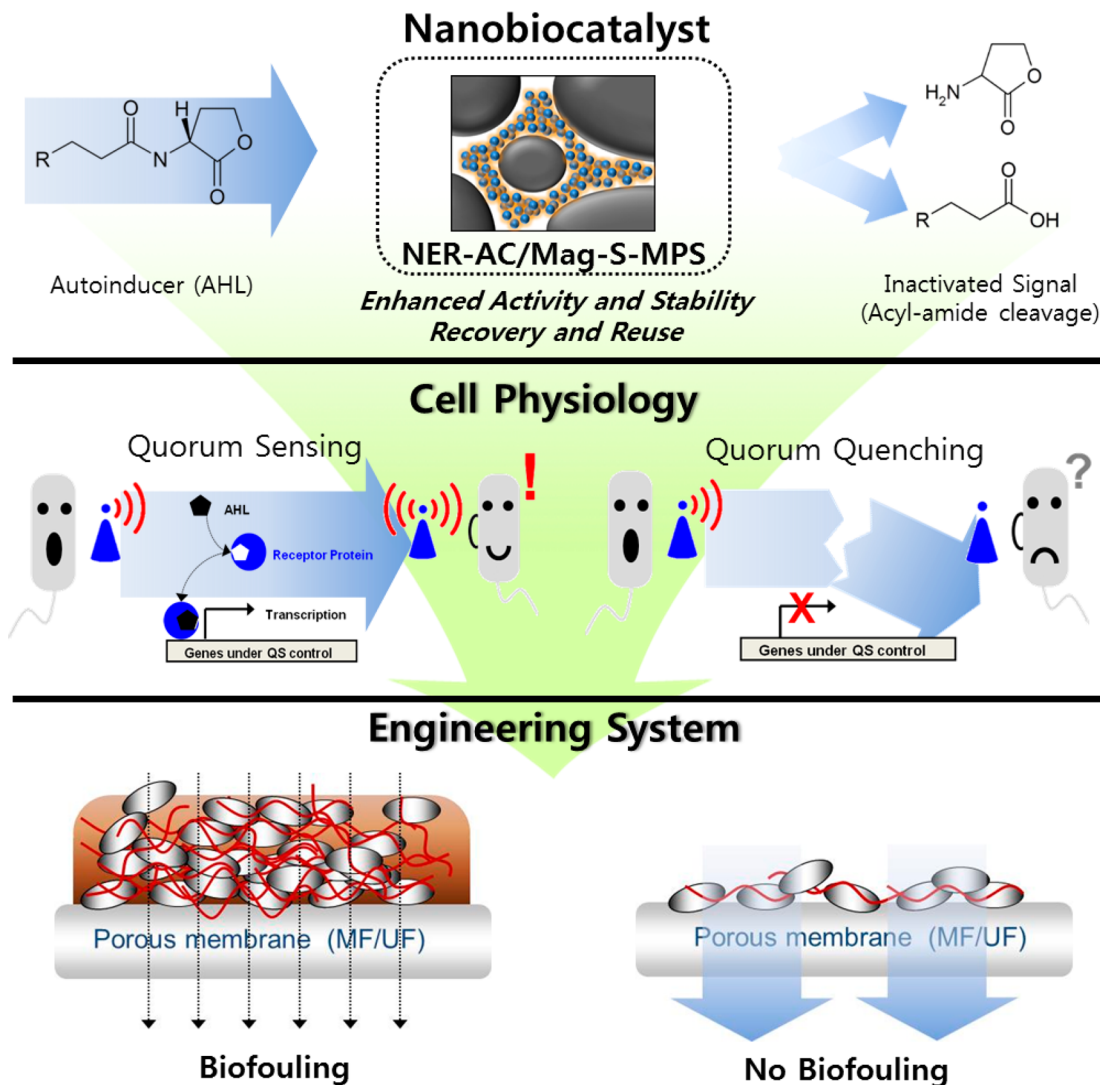
extent.^{11–13} However, the antifouling approach using quorum-quenching enzymes is still at its primitive stage because the enzyme inactivation can lead to a failure of enzymatic antifouling.¹⁴ Therefore, the development of stable enzyme systems is required for the successful application of quorum-quenching enzymes in antifouling.

Nanobiocatalysis, immobilizing and stabilizing enzymes using nanostructured materials, has demonstrated its successes in enhancing the stability as well as loading (apparent activity) of enzymes.^{15,16} Enzymes have been immobilized in various nanomaterials, such as mesoporous materials, nanoparticles, nanofibers, nanotubes, and combined materials of those. High enzyme loading could be easily achieved by controlling the nanostructure, providing high pore volume or large surface area for the enzyme immobilization. By employing the approach of enzyme cross-linking while immobilizing enzymes, successful enzyme stabilization could also be achieved due to the effective prevention of enzyme leaching as well as denaturation, opening up potentials for stabilized enzymes to be employed in various enzyme applications where the poor enzyme stability prevents

Received: October 30, 2013

Revised: March 5, 2014

Published: March 6, 2014

Scheme 1. Design Concept of Antifouling NER-AC/Mag-S-MPS Platform^a

^aDisrupting quorum sensing signal molecules by using nanobiocatalysts regulate the physiological state of bacterial cells, which finally results in the alleviation of biofilm formation and enhances system performance. NER stabilization maintains enzyme stability in harsh environments. Magnetic nanoparticles are incorporated within the support for recovery and reuse. Commercial spherical mesoporous silica endows economical feasibility by virtue of its mass production.

their successes.^{15,16} The potential applications of nanobiocatalysts have been successfully demonstrated in various fields, such as biosensors,^{17,18} biofuel cells,^{19,20} biodiesel production,²¹ proteomics,²² enzyme linked immunosorbent assay (ELISA),^{23,24} and antifouling.¹³ As an example of antifouling nanobiocatalysts, carbon nanotubes conjugated with protease and cell-wall degrading lysostaphin showed good antifouling performance by delaying microbial attachment and killing antibiotic-resistant pathogens.²⁵

In the present work, we developed highly effective antifouling platform by immobilizing quorum-quenching enzyme (acylase, AC) into magnetically separable mesoporous silica (Mag-S-MPS) via a two-step process of enzyme adsorption and cross-linking. The activity of the cross-linked acylase molecules in Mag-S-MPS, called “nanoscale enzyme reactors” (NERs), were effectively stabilized due to the combination of two different mechanisms. One is the prevention of enzyme denaturation due to multipoint covalent linkages on the enzyme surface that are formed upon enzyme cross-linking, while the other is a

“ship-in-a-bottle” mechanism that effectively inhibits the leaching of cross-linked enzymes through the bottleneck mesoporous structure of Mag-S-MPS.^{26–28} To meet the scale requirement of mesoporous silica (MPS) for successful application of NERs in a large scale process of antifouling, we selected commercially available MPS in spherical form (S-MPS), and magnetic nanoparticles were preincorporated into S-MPS for facile magnetic separation.^{29,30} Highly stable, active, and magnetically separable NER-AC in Mag-S-MPS (NER-AC/Mag-S-MPS) was tested for its antifouling properties in membrane filtration for water treatment in the presence of model microorganisms, *Pseudomonas aeruginosa* (Scheme 1).

MATERIALS AND METHODS

Materials. Acylase (EC.3.5.1.14, hydrolase from porcine kidney), N-acetyl-L-methionine, L-methionine, sodium phosphate monobasic, sodium phosphate dibasic, Tris-HCl, Trizma base, glutaraldehyde (GA), o-phthalidialdehyde (OPA), and 2-mercaptoethanol were purchased from Sigma (St. Louis, MO, U.S.A.). A bicinchoninic acid (BCA) protein assay kit was obtained from Pierce (Rockford, IL,

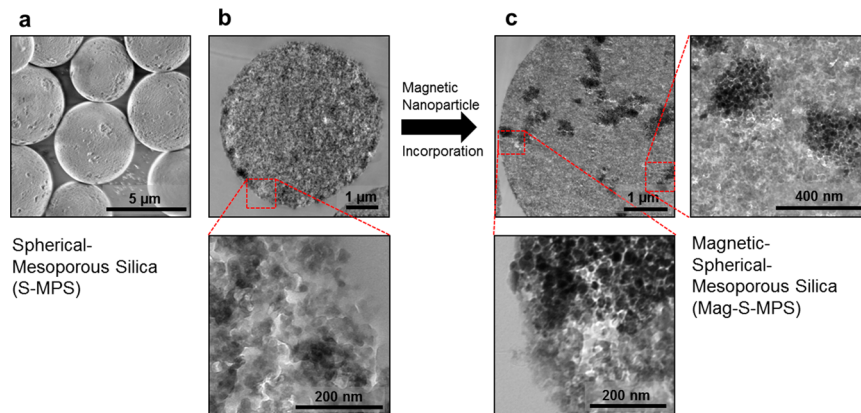


Figure 1. (a) SEM and (b) TEM images of S-MPS ($5\text{ }\mu\text{m}$). (c) TEM images of Mag-S-MPS ($5\text{ }\mu\text{m}$).

U.S.A.). Spherical mesoporous silica (S-MPS) was purchased from Orochem (Lombard, IL, U.S.A.). The other chemicals and materials were purchased from Aldrich (Milwaukee, WI, U.S.A.).

Preparation and Characterization of Magnetic Nanoparticles Incorporated Spherical Mesoporous Silica (Mag-S-MPS). To prepare magnetically separable mesoporous silica (Mag-S-MPS), $\text{Fe}(\text{NO}_3)_3 \cdot 9\text{H}_2\text{O}$ (3.45 g) was dissolved in ethanol (40 mL), and spherical mesoporous silica (2 g) was then added. The solution was stirred at room temperature until all the solvent was removed. Final material with a dark brown color was obtained after heat-treatment at $400\text{ }^\circ\text{C}$ under a flowing argon (95%)/hydrogen (5%) gas mixture. The magnetic nanoparticles aggregated prior to this into mesopores by anisotropic dipole–dipole interactions between superparamagnetic nanoparticles, even in the absence of an applied magnetic field.^{31,32}

The surface areas of the prepared samples were calculated from their 77 K N_2 adsorption–desorption isotherms by using a Tristar II 3020 system (Micromeritics Inc.) according to the Brunauer–Emmett–Teller (BET) method. The pore size distribution was obtained from the adsorption branch by using the Barrett–Joyner–Halenda (BJH) method. The structure of materials was examined by field emission scanning electron microscopy (FESEM, Hitachi S-4800). Transmission electron microscopic images were obtained on a transmission electron microscope (TEM, Hitachi H-7600) operated at 100 kV. Powder X-ray diffraction (XRD) patterns were obtained with a Rigaku D/Max-2500 diffractometer using $\text{Cu K}\alpha$ radiation ($\lambda = 1.5418\text{ \AA}$) at a scanning rate of $4.00^\circ\text{ min}^{-1}$. Magnetizations were determined using a commercial SQUID magnetometer (MPMS 5XL, Quantum Design).

Immobilization of Acylase in Mag-S-MPS. Acylase (AC) was dissolved in sodium phosphate buffer (10 mM, pH 7.0) to prepare a 2 mg/mL enzyme solution. Mag-S-MPS (10 mg) was mixed with 1.5 mL of enzyme solution, and the mixture was incubated on a rocking chair (50 rpm) at room temperature for 20 min for the adsorption of AC into Mag-S-MPS (ADS-AC/Mag-S-MPS). NER-AC/Mag-S-MPS was prepared by further treatment with a 0.1% GA solution in phosphate buffer (100 mM sodium phosphate buffer, pH 7.0) under shaking (200 rpm) for 2 h. Both samples (ADS-AC and NER-AC) were washed using phosphate buffer (100 mM sodium phosphate buffer, pH 7.0) and incubated in 100 mM Tris-HCl (pH 7.0) under shaking (200 rpm) for 30 min to cap the unreacted aldehyde groups. Finally, ADS-AC and NER-AC were washed extensively using a buffer solution (10 mM sodium phosphate buffer, pH 7.0), and stored in the same buffer at $4\text{ }^\circ\text{C}$ until use.

Measurement of Enzyme Activity and Stability. The activity of acylase was quantitatively measured by a fluorometric method using o-phthalaldehyde (OPA), which reacted with the amino group of L-methionine from the AC-catalyzed hydrolysis of *N*-acetyl-L-methionine. Upon reaction with L-methionine, OPA formed fluorescent moieties in conjunction with the reduced sulphydryl group, which enhanced the sensitivity of the AC assay when compared to a

conventional spectrophotometric method using absorbance at 238 nm for the measurement of the generated L-methionine (Figure S3).

A sample solution (1 mL) containing ADS-AC or NER-AC (0.5 mg/mL) was mixed with the same volume of *N*-acetyl-L-methionine solution (10 mM in phosphate buffer). Then, a 0.15 mL aliquot was taken from the reaction solution at the appropriate time and added to the 1.5 mL of OPA solution (0.1 mg/mL of OPA in 50 mM sodium borate buffer, pH 9.5) with 1.35 mL of 100 mM phosphate buffer. Upon excitation at $\lambda_{\text{ex}} = 340\text{ nm}$, the emission intensity at $\lambda_{\text{em}} = 455\text{ nm}$ was measured using a spectrofluorophotometer (RF-5301, Shimadzu, Japan). The reaction rate was calculated from the time-dependent increase in emission intensity.

The stability of the samples was checked under rigorous shaking as described elsewhere.^{26,27} Briefly, each sample in phosphate buffer was shaken horizontally at 200 rpm, and an aliquot was time-dependently withdrawn for the measurement of residual activity as described above. The relative activity at each time point was calculated using the ratio of residual activity to the initial activity of each sample. To check the amount of leached enzyme during the stability experiment, the protein amount in the solution after magnetic separation was measured by using BCA assay.

Biofilm Growth on a Membrane Filter. A culture of *Pseudomonas aeruginosa* (*P. aeruginosa*) PAO1 expressing a green fluorescent protein (GFP) was grown at $30\text{ }^\circ\text{C}$ overnight in Luria–Bertani (LB) broth. For biofilm growth on a membrane, total 48 polyvinylidene fluoride (PVDF) membrane disk filters with a pore size of $0.45\text{ }\mu\text{m}$ (Millipore, U.S.A.) were attached onto the sterile slide glass and placed into a 50 mL conical tube with 49 mL of synthetic wastewater, the composition of which was described in a previous study.¹² Then, 1 mL of GFP-tagged *P. aeruginosa* PAO1 was inoculated into the conical tube and incubated under shaking condition (150 rpm) at room temperature for 24 days. The synthetic wastewater was daily replaced with fresh water to maintain biofilm growth on each membrane filter. During each day, two samples were taken for the purpose of performing filterability tests and making biofilm observations, respectively.

Measurement of Membrane Permeability. Fouling of the membrane filter by the biofilm was quantitatively evaluated by measuring the loss of water permeability level. In detail, 50 mL of distilled water was placed in the stirred cell (Amicon, Model 8400, U.S.A.) with the biofilm sample and the water flux was determined under a constant pressure of 10 kPa by using nitrogen gas. The relative permeability at each time point was calculated using the ratio of the residual flux to the initial flux for each membrane sample.

Confocal Laser Scanning Microscopy (CLSM). The biofilms of GFP-tagged *P. aeruginosa* PAO1 that formed on the membrane filter were visually monitored using CLSM (Nikon C1 plus, Japan) without further fluorescent staining. Images were obtained with a $60\times$ objective lens and recorded in green channel (excitation at $\lambda_{\text{ex}} = 488\text{ nm}$ and emission at $\lambda_{\text{em}} = 515/30\text{ nm}$). A Z-section image stack consisting of

three-dimensional images was constructed using IMARIS software (Bitplane AG, Zurich, Switzerland).

RESULTS AND DISCUSSION

Preparation of Mag-S-MPS and Acylase Immobilization. To meet the demand for a large quantity of immobilization carriers in a large-scale antifouling process, we have selected commercially available mesoporous silica in a spherical form (S-MPS) (Figure 1a,b). Magnetic nanoparticles were incorporated into the S-MPS to prepare Mag-S-MPS (Figure 1c), allowing for facile magnetic separation of immobilized enzymes. As shown in the transmission electron microscopy (TEM) images, S-MPS (5 μm diameter) was synthesized by the aggregation of silica nanoparticles, and the mesopores of S-MPS (median mesopores of 34 nm; see Figure S1) represent interparticle space of silica nanoparticles upon aggregation. After incorporation of magnetic nanoparticles, the surface area and pore volume were reduced from $110 \pm 1 \text{ m}^2/\text{g}$ and $0.66 \pm 0.02 \text{ cm}^3/\text{g}$ (S-MPS) to $45 \pm 1 \text{ m}^2/\text{g}$ and $0.37 \pm 0.02 \text{ cm}^3/\text{g}$ (Mag-S-MPS), respectively, while the median pore size of 34 nm was not changed (Figure S1). Mag-S-MPS still has a sufficient pore volume to accommodate a large quantity of enzymes. Mag-S-MPS exhibits a superparamagnetic property with a mass magnetization value of 10.85 emu/g (Figure S2), thereby allowing for facile magnetic separation and easy redispersion during the iterative washing and recycling of Mag-S-MPS with immobilized enzymes.²⁹

Acyrase (AC) was immobilized into Mag-S-MPS via two different approaches: simple adsorption (ADS-AC) and a two-step process consisting of enzyme adsorption and cross-linking, called “nanoscale enzyme reactors” of AC (NER-AC).^{21,26,39} The adsorption of AC into Mag-S-MPS was completed in 20 min, with a final enzyme loading of $2.8 \pm 0.1 \text{ wt } \%$. When considering the theoretically maximum enzyme loading of ADS-AC to be 3.9 wt % (see detailed calculation in Supporting Information), most mesopores in Mag-S-MPS were readily available for the adsorption of acylase ($13.45 \text{ nm} \times 13.45 \text{ nm} \times 7.45 \text{ nm}$),³³ and the difference can be explained by imperfect packing and mesopores that were not available for enzyme adsorption. ADS-AC is simple to prepare, but could not prevent the leaching of enzymes from Mag-S-MPS. The poor enzyme stability of ADS-AC due to the enzyme leaching would inhibit its practical use in industrial bioprocess where the long-term stability of enzyme performance is required. As a potential solution, NER-AC was prepared by simply cross-linking enzyme molecules after the step of enzyme adsorption. NER-AC can potentially improve the enzyme stability if the cross-linked enzymes can be effectively entrapped in the mesopores of Mag-S-MPS as shown in Figure 2a. The use of Mag-S-MPS enables facile magnetic separation for the repeated uses of NER-AC (Figure 2b).

Activity and Stability of Acylase Immobilized Mag-S-MPS. The activities of free AC, ADS-AC, and NER-AC were measured via a fluorometric assay using *o*-phthaldialdehyde (OPA). According to a conventional AC assay, the AC activity is measured by the decrease of A238, which results from the enzymatic hydrolysis of *N*-acetyl-L-methionine into acetic acid and L-methionine.³⁴ Despite of its simplicity, however, this spectrophotometric assay can be interfered by other chemicals that also exhibit absorbance at 238 nm, such as L-methionine, leading to a low detection limit. In the present work, we employed the OPA assay, in which OPA reacts with free amino groups and generates the fluorescence signal.³⁵ Because the

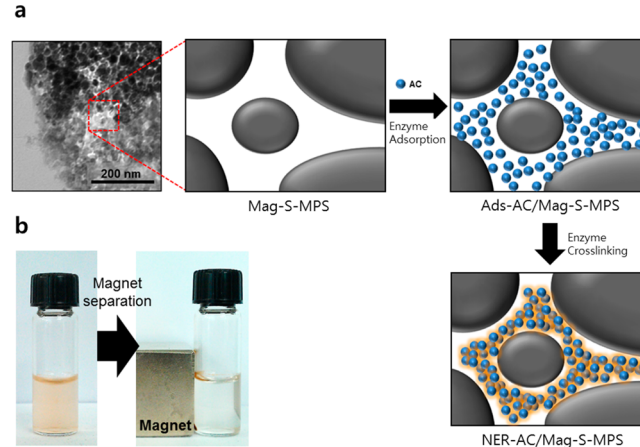


Figure 2. (a) Schematic illustrations for the preparation of nanoscale enzyme reactors of acylase in Mag-S-MPS. (b) Magnetic capture of NER-AC/Mag-S-MPS.

AC-catalyzed hydrolysis of *N*-acetyl-L-methionine produces L-methionine with free amino groups, the OPA assay can report the enzymatic hydrolysis in form of fluorescence signal by the reaction of OPA with L-methionine. By using free AC, we performed the hydrolytic reaction of *N*-acetyl-L-methionine in aqueous buffer (50 mM sodium borate, pH 9.5) and measured the AC activity in various concentrations (Figure S4).

The specific activities of free AC, ADS-AC, and NER-AC were 9.033 ± 0.015 , 1.338 ± 0.020 , and $1.654 \pm 0.006 \text{ mM h}^{-1}$ per mg of enzyme, representing that ADS-AC and NER-AC resulted in 15 and 18% specific activities, respectively, when compared to that of free AC. This can be explained by the enzyme inactivation during immobilization and limitation against the transfer of substrate during the enzyme reaction. The specific activity of NER-AC was 1.2× higher than that of ADS-AC, which is also explained by the enzyme inactivation and mass-transfer limitation.²⁶ In other words, the specific activity of NER-AC is higher than that of ADS-AC due to the prevention of enzyme inactivation.²⁷

The stabilities of free AC, ADS-AC, and NER-AC were checked by measuring the AC activity time dependently after incubation in an aqueous buffer (50 mM sodium borate, pH 9.5) under shaking (200 rpm) at room temperature. In a typical bioprocess with immobilized enzymes, rigorous shaking is required to reduce the mass transfer limitation, and it is highly desirable to maintain the enzyme activity under shaking for the successful application of immobilized enzymes. Figure 3 shows the stabilities of free AC, ADS-AC, and the relative activity represents the ratio of residual activity at each time point to the initial activity of each sample. Free AC showed a rapid decrease of AC activity due the enzyme inactivation via denaturation and autolysis. ADS-AC stabilized the AC activity when compared to free AC, but also showed a monotonous decrease of AC activity due to continuous enzyme leaching and follow-up AC inactivation via denaturation and autolysis (Figure S5). On the other hand, NER-AC showed a good stabilization of AC activity even under rigorous shaking condition (200 rpm). Free AC showed less than 5% of its initial activity after two days while the relative activities of ADS-AC and NER-AC after 1 month incubation under shaking were 3 and 82%, respectively. Higher stability of NER-AC was mainly derived by the ship-in-a-bottle mechanism that effectively inhibits the leaching of cross-linked enzymes from the mesopore structure of Mag-S-

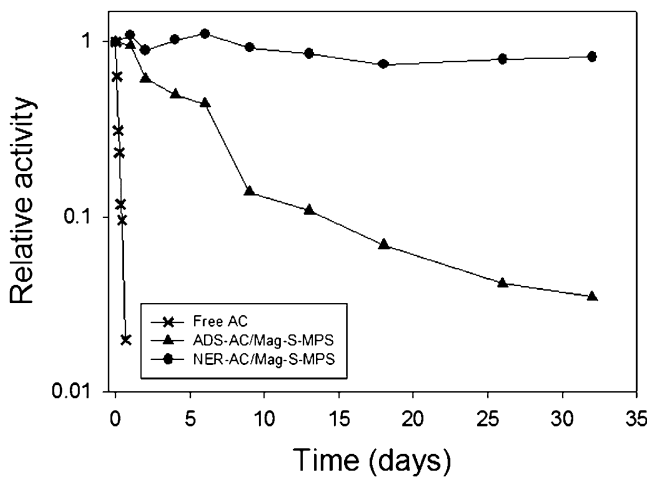


Figure 3. Stability of free AC, ADS-AC/Mag-S-MPS, and NER-AC/Mag-S-MPS under shaking (200 rpm).

MPS. In other words, once enzyme molecules are cross-linked, the resulting cross-linked enzymes can be entangled with the silica nanoparticles and mesopores of Mag-S-MPS, which resulted in an effective prevention of enzyme leaching from Mag-S-MPS. Actually, the ship-in-a-bottle mechanism of NER approach was first proposed by using the mesoporous silica with bottleneck mesopore structure.²⁶ Recently, we also demonstrated the success of NER approach by using mesostructured onion-like silica that effectively prevents the leaching of cross-linked enzymes in mesoporous channels with high aspect ratio.²¹ In the present work, our stabilization result of NER-AC in Mag-S-MPS represents another new success of NER approach by using commercial MPS that can be produced in a large scale and have internanoparticles space as mesopores.

Antifouling of NER-AC in Membrane. We checked the potential application of highly stable NER-AC for the membrane antifouling in the model system of water treatment. Polyvinylidene fluoride (PVDF) was selected as a model membrane because it is adopted in most of commercial membrane processes due to its good resistance to chemicals such as chlorine.³⁶ NER-AC was added to the container with membrane, where *P. aeruginosa* PAO1 was incubated in the synthetic wastewater with extremely high organic loadings. This model system was designed to observe the biofilm formation over a reasonably short period of time. Time-dependently, we removed the membrane from the container, and measured the permeability of membrane that represents the water flux under the pressure of 10 KPa. The antifouling efficiency was quantitatively determined in terms of relative permeability, which is the ratio of water flux at a specific time to initial water flux of each sample. Two control cases of “no addition of NER-AC” and “addition of Mag-S-MPS” showed a rapid drop of relative permeability after incubation for six days, while the relative permeability of membrane after 14-day incubation in presence of NER-AC did not show a rapid drop and maintained reasonable permeability with no serious plugging of membrane (Figure 4). The general biofilm cycle consists of attachment of single cells, colonization, and then development a complex biofilm structure with a polymer matrix. In particular, high density microcolonies differentiate into mature biofilm via a QS-dependent mechanism, which results in an abrupt increase in biofouling in membrane processes.^{37,38} In the present result, the relative permeability of both control

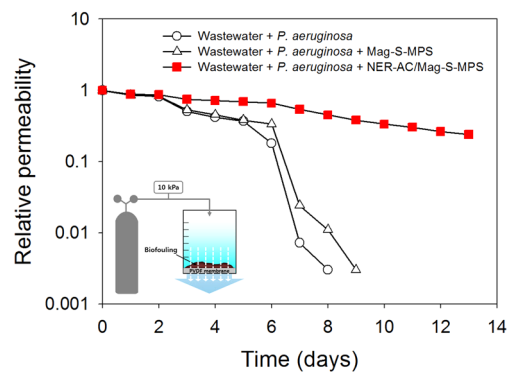


Figure 4. Antifouling with NER-AC/Mag-S-MPS in membrane filtration.

experiments without AC declined abruptly in 6–8 days, which is similar to general biofouling profiles in conventional membrane filtration, that is, an initially slow and gradual increase followed by an abrupt rise in fouling.¹² The antifouling effect of NER-AC, as demonstrated in reasonable permeability and no plugging of membrane, can be interpreted as a result of AC-catalyzed QS quenching.

To check the effect of NER-AC on biofilm development, we examined the confocal laser scanning microscopy (CLSM) images on the surface of the membrane obtained in the same condition for the experiment to obtain the relative permeability (Figure 4). Figure 5 shows that NER-AC effectively prevented the transition from surface colonization to a mature complex structure in the form of biofilm. On the other hand, two controls with no acylase addition showed rapid maturation of their biofilms. In the present work, the chemical oxygen demand (COD) concentration of synthetic wastewater was 1000 mg/L to accelerate the antifouling effect within a reasonable time. When considering a much lower COD concentration (150–300 mg/L) in real municipal wastewaters, the present results of NER-AC can be easily translated to the practical success in antifouling for water treatment system.

It is worthy to note that NER-AC successfully alleviated biofilm maturation on the surface, which enhanced the membrane permeability at a very low effective dosage level of 0.5 mg/L. This is 1 order of magnitude lower level than that of previous studies with the same synthetic wastewater, free enzyme, and a conventional enzyme stabilization support of commercial magnetically separable ion-exchange resin.^{12,13} This implies that NER-AC could be a promising solution to enzyme applications in the environmental field where economic feasibility as well as performance is important.

CONCLUSIONS

We have developed an effective antifouling system by immobilizing and stabilizing quorum-quenching acylase in magnetically separable mesoporous silica, which can be produced in a large scale. Highly stable and magnetically separable NER-AC can be easily fabricated with commercial components and maintains its antifouling activity for a long time, both of which are essential characteristics for industrial scale application under continuous operation such as for membrane filtration in the water treatment. As an example of antifouling in engineering process, NER-AC was proven to effectively alleviate the biofilm maturation of *P. aeruginosa* PAO1 on a membrane surface and thereby enhanced its filtration performance even under harsh conditions of high

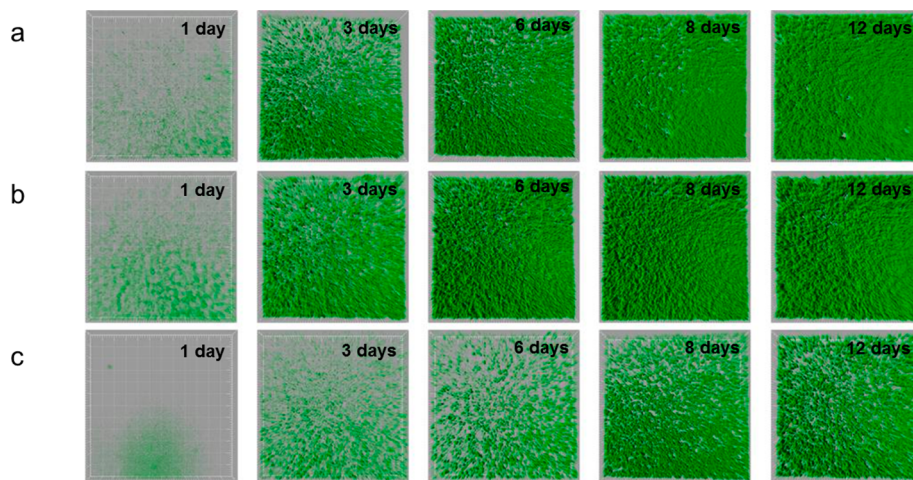


Figure 5. Confocal images of *P. aeruginosa* PAO1 biofilm development on the membrane surface during the growth of (a) control, (b) Mag-S-MPS, and (c) NER AC/Mag-S-MPS (each image covers an area of $1214 \times 1214 \mu\text{m}^2$).

organic loading and low enzyme dosage level. As a result, synergy between the enzymatic regulation of basic microbial signaling and nanobiocatalytic enzyme stabilization proves its high potential as a simple and effective antifouling solution in various areas.

ASSOCIATED CONTENT

Supporting Information

Pore size distributions of S-MPS and Mag-S-MPS, magnetic property of Mag-S-MPS, reaction scheme and activity measurement of *o*-phthalodialdehyde (OPA) fluorometry for acylase, enzyme leaching of ADS and NER-AC/Mag-S-MPS, and calculation of theoretically maximum acylase loading amount in Mag-S-MPS. This material is available free of charge via the Internet at <http://pubs.acs.org>.

AUTHOR INFORMATION

Corresponding Author

*Tel.: +82-2-3290-4850. Fax: +82-2-925-4850. E-mail: jbkim3@korea.ac.kr.

Author Contributions

†These authors contributed equally (B.L. and K.-M.Y.).

Notes

The authors declare no competing financial interest.

ACKNOWLEDGMENTS

This work was supported by “International Collaborative R&D Program” of the Korea Institute of Energy Technology Evaluation and Planning (KETEP) grant funded by the Korea government Ministry of Trade, Industry and Energy (20118510020020) and the National Research Foundation of Korea (NRF) grant funded by the Korea government Ministry of Science, ICT and Future Planning (2013K000229 and 2014 University-Institute Cooperation Program).

REFERENCES

- (1) Wisniewski, N.; Moussy, F.; Reichert, W. M. *Fresenius' J. Anal. Chem.* **2000**, *366*, 611–621.
- (2) Hallam, N. B.; West, J. R.; Forster, C. F.; Simms, J. *Water Res.* **2001**, *35*, 4063–4071.
- (3) Costerton, J. W.; Montanaro, L.; Arciola, C. R. *Int. J. Artif. Organs* **2005**, *28*, 1062–1068.
- (4) Qian, P. Y.; Lau, S. C. K.; Dahms, H. U.; Dobretsov, S.; Harder, T. *Mar. Biotechnol.* **2007**, *9*, 399–410.
- (5) Parsek, M. R.; Greenberg, E. P. *Trends Microbiol.* **2005**, *13*, 27–33.
- (6) Davies, D. G.; Parsek, M. R.; Pearson, J. P.; Iglesias, B. H.; Costerton, J. W.; Greenberg, E. P. *Science* **1998**, *280*, 295–298.
- (7) Hentzer, M.; Wu, H.; Andersen, J. B.; Riedel, K.; Rasmussen, T. B.; Bagge, N.; Kumar, N.; Schembri, M. A.; Song, Z. J.; Kristoffersen, P.; Manefield, M.; Costerton, J. W.; Molin, S.; Eberl, L.; Steinberg, P.; Kjelleberg, S.; Hoiby, N.; Givskov, M. *EMBO J.* **2003**, *22*, 3803–3815.
- (8) Surette, M. G.; Bassler, B. L. *Proc. Natl. Acad. Sci. U.S.A.* **1998**, *95*, 7046–7050.
- (9) Waters, C. M.; Bassler, B. L. *Annu. Rev. Cell Dev. Biol.* **2005**, *21*, 319–346.
- (10) Bassler, B. L. *Curr. Opin. Microbiol.* **1999**, *2*, 582–587.
- (11) Kim, J. H.; Choi, D. C.; Yeon, K. M.; Kim, S. R.; Lee, C. H. *Environ. Sci. Technol.* **2011**, *45*, 1601–1607.
- (12) Yeon, K. M.; Cheong, W. S.; Oh, H. S.; Lee, W. N.; Hwang, B. K.; Lee, C. H.; Beyenal, H.; Lewandowski, Z. *Environ. Sci. Technol.* **2009**, *43*, 380–385.
- (13) Yeon, K. M.; Lee, C. H.; Kim, J. *Environ. Sci. Technol.* **2009**, *43*, 7403–7409.
- (14) Judd, S.; Judd, C. *The MBR Book: Principles and Applications of Membrane Bioreactors in Water and Wastewater Treatment*; Elsevier Limited: Oxford, 2011.
- (15) Kim, J.; Grate, J. W.; Wang, P. *Chem. Eng. Sci.* **2006**, *61*, 1017–1026.
- (16) Kim, J.; Grate, J. W.; Wang, P. *Trends Biotechnol.* **2008**, *26*, 639–646.
- (17) Heilmann, A.; Teuscher, N.; Kiesow, A.; Janasek, D.; Spohn, U. *J. Nanosci. Nanotechnol.* **2003**, *3*, 375–379.
- (18) Lee, D.; Lee, J.; Kim, J.; Kim, J.; Na, H. B.; Kim, B.; Shin, C. H.; Kwak, J. H.; Dohnalkova, A.; Grate, J. W.; Hyeon, T.; Kim, H. S. *Adv. Mater.* **2005**, *17*, 2828–2833.
- (19) Fischbeck, M. B.; Youn, J. K.; Zhao, X. Y.; Wang, P.; Park, H. G.; Chang, H. N.; Kim, J.; Ha, S. *Electroanalysis* **2006**, *18*, 2016–2022.
- (20) Fischbeck, M.; Kwon, K. Y.; Lee, I.; Shin, S. J.; Park, H. G.; Kim, B. C.; Kwon, Y.; Jung, H. T.; Kim, J.; Ha, S. *Biotechnol. Bioeng.* **2012**, *109*, 318–324.
- (21) Jun, S. H.; Lee, J.; Kim, B. C.; Lee, J. E.; Joo, J.; Park, H.; Lee, J. H.; Lee, S. M.; Lee, D.; Kim, S.; Koo, Y. M.; Shin, C. H.; Kim, S. W.; Hyeon, T.; Kim, J. *Chem. Mater.* **2012**, *24*, 924–929.
- (22) Kim, B. C.; Lopez-Ferrer, D.; Lee, S. M.; Ahn, H. K.; Nair, S.; Kim, S. H.; Kim, B. S.; Petritis, K.; Camp, D. G.; Grate, J. W.; Smith, R. D.; Koo, Y. M.; Gu, M. B.; Kim, J. *Proteomics* **2009**, *9*, 1893–1900.
- (23) Piao, Y.; Lee, D.; Kim, J.; Kim, J.; Hyeon, T.; Kim, H. S. *Analyst* **2009**, *134*, 926–932.

- (24) Piao, Y.; Lee, D.; Lee, J.; Hyeon, T.; Kim, J.; Kim, H. S. *Biosens. Bioelectron.* **2009**, *25*, 906–912.
- (25) Miao, J. J.; Pangule, R. C.; Paskaleva, E. E.; Hwang, E. E.; Kane, R. S.; Linhardt, R. J.; Dordick, J. S. *Biomaterials* **2011**, *32*, 9557–9567.
- (26) Lee, J.; Kim, J.; Jia, H. F.; Kim, M. I.; Kwak, J. H.; Jin, S. M.; Dohnalkova, A.; Park, H. G.; Chang, H. N.; Wang, P.; Grate, J. W.; Hyeon, T. *Small* **2005**, *1*, 744–753.
- (27) Kim, M. I.; Kim, J.; Lee, J.; Jia, H.; Bin Na, H.; Youn, J. K.; Kwak, J. H.; Dohnalkova, A.; Grate, J. W.; Wang, P.; Hyeon, T.; Park, H. G.; Chang, H. N. *Biotechnol. Bioeng.* **2007**, *96*, 210–218.
- (28) Kim, M. I.; Kim, J.; Lee, J.; Shin, S.; Bin Na, H.; Hyeon, T.; Park, H. G.; Chang, H. N. *Microporous Mesoporous Mater.* **2008**, *111*, 18–23.
- (29) Lee, J.; Bin Na, H.; Kim, B. C.; Lee, J. H.; Lee, B.; Kwak, J. H.; Hwang, Y.; Park, J. G.; Gu, M. B.; Kim, J.; Joo, J.; Shin, C. H.; Grate, J. W.; Hyeon, T. *J. Mater. Chem.* **2009**, *19*, 7864–7870.
- (30) Hwang, E. T.; Lee, B.; Zhang, M.; Jun, S. H.; Shim, J.; Lee, J.; Kim, J.; Gu, M. B. *Green Chem.* **2012**, *14*, 1884–1887.
- (31) Ge, J. P.; Hu, Y. X.; Biasini, M.; Beyermann, W. P.; Yin, Y. D. *Angew. Chem., Int. Ed.* **2007**, *46*, 4342–4345.
- (32) Varon, M.; Pena, L.; Balcells, L.; Skumryev, V.; Martinez, B.; Puntes, V. *Langmuir* **2010**, *26*, 109–116.
- (33) Zhao, H. Y.; Meng, W. Y.; Lin, Z. J.; Zhou, H. M. *Chin. Sci. Bull.* **1997**, *42*, 1750–1752.
- (34) Mitz, M. A.; Schlueter, R. J. *Biochim. Biophys. Acta* **1958**, *27*, 168–172.
- (35) Dean, K. E. S.; Klein, G.; Renaudet, O.; Reymond, J. L. *Bioorg. Med. Chem. Lett.* **2003**, *13*, 1653–1656.
- (36) Yang, W. B.; Cicek, N.; Ilg, J. *J. Membr. Sci.* **2006**, *270*, 201–211.
- (37) Parsek, M. R.; Greenberg, E. P. *Proc. Natl. Acad. Sci. U.S.A.* **2000**, *97*, 8789–8793.
- (38) Fuqua, C.; Greenberg, E. P. *Nat. Rev. Mol. Cell Biol.* **2002**, *3*, 685–695.